Research Article | Vol. 26, No. 16 | 6 Aug 2018 | OPTICS EXPRESS 19750

Optics EXPRESS

Space-time multichannel adaptive filtering scheme for VLC color cross-talk equalization

Stefano Pergoloni, Mauro Biagi,* Roberto Cusani, and Gaetano Scarano

Department of Information, Electrical and Telecommunication (DIET) Engineering, "La Sapienza" University of Rome, Via Eudossiana 18, 00184 *Rome, Italy*
Mauro.Biagi@uniroma1.it

Abstract: In the emerging framework of visible light communications, the limitation of modulation bandwidth of light emitting diodes (LEDs) transmitters is counterbalanced by the use of red-green-blue (RGB) LEDs since they exhibit higher modulation bandwidth. Using RGB LEDs allows to exploit the spatial multiplexing aspects, that is obtaining parallel channels for transmission. In this context, we used at the receiver RGB-tuned photodiodes (PDs). Hence each PD can, in principle, detect only the information its tuning is matched to. The drawback of increasing spectral efficiency is the presence of cross-talk at the single PD due to the signals emitted by the remaining colors when a perfect color filtering is not applied. In this paper we consider amplitude shift keying (ASK) modulation, investigate the issue of the spatial (color) interference and we present a blind multichannel adaptive equalizer able to mitigate the temporary intersymbol interference (ISI) and also the spatial (color) ISI, this latter partially suppressed using suitable color filters. We analyze also the convergence of the adaptive algorithm and compare its performance with the literature.

OCIS codes: (060.2605) Free-space optical communication; (060.4080) Modulation.

References and links

1. T. Komine and M. Nakagawa, "Fundamental analysis for visible-light communication system using LED lights," IEEE Transactions on Consumer Electronics **50**(1), 100–107 (2004).
2. S. Pergoloni, M. Biagi, S. Colonnese, R. Cusani and G. Scarano, "Optimized LEDs Footprinting for Indoor Visible Light Communication Networks", IEEE Photonics Technology Letters, **28**(4), 532–535 (2016).
3. H. Chun, S. Rajbhandari, G. Faulkner, D. Tsonev, E. Xie, J.J.D. McKendry, E. Gu, M.D. Dawson, D.C. O'Brien and H. Haas, "LED Based Wavelength Division Multiplexed 10 Gb/s Visible Light Communications", IEEE Journal of Lightwave Technology, **34**(13), 3047–3052 (2016).
4. IEEE Std 802.15.7-2011, IEEE Standard for Local and Metropolitan Area Networks–Part 15.7: Short-Range Wireless Optical Communication Using Visible Light, pp.1–309, (2011)
5. R. Singh, T. O'Farrell, and J. David, "Performance evaluation of IEEE 802.15.7 CSK physical layer", IEEE Globecom Workshops, 1064–1069 (2013).
6. S.Pergoloni, M. Biagi, S. Rinauro, S. Colonnese, R. Cusani, and G. Scarano, "Merging Color Shift Keying and Complementary Pulse Position Modulation for Visible Light Illumination and Communication" IEEE/OSA Journal of Lightwave Technology, **33**(1), 192–200 (2015).
7. Q. Gao, C. Gong, and Z. Xu, "Joint Transceiver and Offset Design for Visible Light Communications With Input-Dependent Shot Noise", IEEE Transactions on Wireless Communications, **16**(5), 2736–2747 (2017).
8. S. Pergoloni, A. Petroni, T.-C. Bui, G. Scarano, R. Cusani, and M. Biagi, "ASK-based spatial multiplexing RGB scheme using symbol-dependent self-interference for detection", Opt. Express **25**(13), 15028–15042 (2017)
9. F. M. Wu, C. T. Lin, C. C. Wei, C. W. Chen, Z. Y. Chen and K. Huang, "3.22-Gb/s WDM Visible Light Communication of a Single RGB LED Employing Carrier-Less Amplitude and Phase Modulation," in Optical Fiber Communication Conference/National Fiber Optic Engineers Conference, OSA Technical Digest (Optical Society of America, 2013)
10. Y. Wang, L. Tao, X. Huang, J. Shi and N. Chi, "Enhanced Performance of a High-Speed WDM CAP64 VLC System Employing Volterra Series-Based Nonlinear Equalizer", in IEEE Photonics Journal, **7**(3), 1–7, 2015.
11. X. Chen and M. Jiang, "Adaptive Statistical Bayesian MMSE Channel Estimation for Visible Light Communication", IEEE Transactions on Signal Processing, **65**(5), 1287–1299 (2017).
12. S. Pergoloni, M. Biagi, S. Colonnese, R. Cusani and G. Scarano, "A Space-Time RLS Algorithm for Adaptive Equalization: The Camera Communication Case", IEEE/OSA Journal of Lightwave Technology, **35**(10), 1811–1820 (2017).

#328142 https://doi.org/10.1364/OE.26.019750
Journal © 2018 Received 11 Apr 2018; revised 12 Jun 2018; accepted 16 Jun 2018; published 23 Jul 2018

Optics EXPRESS

13. M. Biagi and A. M. Vegni and S. Pergoloni and P. M. Butala and T. D. C. Little, "Trace-Orthogonal PPM-Space Time Block Coding Under Rate Constraints for Visible Light Communication", IEEE/OSA Journal of Lightwave Technology, **3**(2), 481–494, 2015.
14. Wiggins, Ralph A. and Robinson, Enders A., 'Recursive solution to the multichannel filtering problem", Journal of Geophysical Research, **70**(8), 1885–1891 (1965).
15. B. Cornelis and M. Moonen and J. Wouters, "Performance Analysis of Multichannel Wiener Filter-Based Noise Reduction in Hearing Aids Under Second Order Statistics Estimation Errors", IEEE Transactions on Audio, Speech, and Language Processing, **19**(5), 1368–1381 (2011).
16. J. R. Barry, J. M. Kahn, W. J. Krause, E. A. Lee, and D. G. Messerschmitt, "Simulation of multipath impulse response for indoor wireless optical channels", IEEE Journal on Selected Areas in Communications, **11**(2), 367-379 (1993).
17. Y. Huang, J. Benesty, Jacob and J. Chen, Acoustic MIMO Signal Processing - Signals and Communication Technology, (Springer-Verlag New York, Inc., Secaucus, NJ, USA, 2006)
18. S. J. Orfanidis, Optimum Signal Processing, (McGraw-Hill, 2007).
19. M. Uysal and F. Miramirkhani and O. Narmanlioglu and T. Baykas and E. Panayirci, "IEEE 802.15.7r1 Reference Channel Models for Visible Light Communications", IEEE Communications Magazine, **55**(1), 212–217 (2017).
20. J. Grubor, S. Randel, K. D. Langer and J. W. Walewski, "Broadband Information Broadcasting Using LED-Based Interior Lighting", IEEE Journal of Lightwave Technology, **26**(4), 3883–3892 (2008).
21. G.Scarano, A. Petroni, M.Biagi, R.Cusani, "Second Order Statistics Driven LMS Blind Fractionally Spaced Channel Equalization", IEEE Signal Processing Letters, **24**(2), 161–163 (2017).
22. J. Fang et al., "An Efficient Flicker-Free FEC Coding Scheme for Dimmable Visible Light Communication Based on Polar Codes", IEEE Photonics Journal, **9**(3), 1–10 (2017).

1. Introduction

Visible light communication (VLC) is a complementary technology to radio frequency that is attracting the international research and industrial community interest [1]. VLC is an optical wireless technology that provides both illumination and communication services. It has several distinctive features in comparison to RF, such as, the unregulated and unlicensed channel (THz of band, visible spectrum), or the opportunity to use indoor LED arrays belonging to the lighting infrastructure. In order to provide higher data rate densities $[Mbit/s/m^2]$ one can resort to spatial reuse or, thanks to the transmitting sources directivity, create very small cells (called atto-cells), both approaches presenting drawbacks like high densification and offloading of the network [2].

In the lighting infrastructure, phospore-based LEDs, also known as white light LEDs (WLEDs), are used; such LEDs are composed by only one LED chip or multi-colored transmitters, e.g. Red-Green-Blue (RGB) LEDs, which are more complex and expensive but have better illumination quality and higher modulation bandwidth in comparison with WLEDs. Another benefit in the adoption of RGB LEDs for VLC is the opportunity to use Wavelength Division Multiplexing (WDM) techniques, in order to improve the system data rate by using the spatial (color) domain as a multiplexing gain [3].

The above reasons have inspired research activities on modulation and system design using multi-colored LEDs, starting by color shift keying that is a flicker-free multicolor VLC scheme specified in the IEEE 802.15.7 physical layer III standard [4] [5] [6], in which the information is mapped into the instantaneous output color of trichromatic LEDs.

However, in WDM multichannel systems the imperfect suppression of the color cross-talk interference can lead to severe bit error rate (BER) degradation. Consequently, as recently presented [7], employing an equalization technique in order to reduce the spatial intersymbol interference is of paramount importance [8].

In the VLC literature, adaptive channel equalization schemes [9] and [10], or channel estimation schemes [11], are implemented in the time-domain only and do not address the issues of color cross-talk. Furthermore, signal pre-equalization and carrierless amplitude phase (CAP) modulation allow the achievement of a 4.5 Gb/s rate by using commercial RGB LEDs and photodiodes [10]. High performance in terms of BER are guaranteed by a Volterra nonlinear equalizer implemented at receiver side in order to compensate the nonlinear behavior of the LED.

Another field in the framework of VLC is the camera communication case. There the spatial aspect is more critical since, due to low frame rate, the space dimension becomes crucial. So

Optics EXPRESS

space-time equalization usually aims at taking into account the spatial dimension by avoiding to manage the time aspect due to the relationship between signaling time and delay spread of the channel [12].

As it appears clear after a deep literature review, some contributions aim at considering channel equalization techniques that exploit the spatial diversity using WLEDs or the color diversity using RGB LEDs. On the other hand, when WLED are used in Single-Input-Single-Output (SISO) configuration, time equalization is taken into account. While space-time coding has been tackled by the literature [13], it is worth noting that space (color) and time aspects, considered as a whole and joint framework, are substantially unexplored from the equalization point of view.

For the above reason, in this work we study and test the use of a multichannel (space-time) equalization in a RGB multiple-input-multiple-output (MIMO) VLC transmission, in order to address the issue raised in [7].

The adoption of multichannel equalizers has a relatively old history, which traces back to the sixties in geophysics field [14] and later on in the acoustic field [15], where typically a high number of receiver arrays are used. However, the here described equalization scheme aims at *solving* the issues of residual cross-talk and temporal ISI, where the term residual cross-talk has to be intended as the color interference not suppressed by the optical filters. Hence we propose an adaptive 3×3 MIMO finite impulse response (FIR) equalizer that acts after the optical (analog) filtering provided by colored lenses placed in front of the PDs. More in detail, each optical filter ideally passes only the contribution coming from the corresponding LED; in such a way, the first PD receives only the contribution from the first LED and so forth. The filter impulse responses belonging to different colors are, in principle, designed with different lengths, i.e. shorter impulse response equalizers are applied to the cross-talk channels where the impulse response is more attenuated by optical filters thus reducing the equalization effort.

We provide simulation results under different VLC channel conditions, highlighting the benefit provided by using a multichannel adaptive filtering scheme. An interesting outcome is that short equalizer filters, which reduces computational complexity, do not degrade the equalization performance especially when the optical filters *sufficiently* mitigate cross-talk. The reminder of paper is organized as follows: in Sect.2 we introduce the system model of the 3x3 MIMO system, in Sect.3 the equalizer is presented and the three equivalent 3×1 MISO system is reported in Sect.3.1 with the discussion of the filter support design. The numerical results are given in Sect.4. Last, the concluding remarks are provided.

2. System model

We consider a VLC system with 3 transmitting colored LEDs and 3 receiving PDs. The discrete signal transmitted from the l-th LED is $a_l[n]$, which represents the transmitted real valued equiprobable and statistically independent (both in time and space) symbols of an M-ary, ASK constellation. Moreover, the symbol period is T_s so the transmission data rate is $(3/T_s)\log_2 M$, that is, three times the data rate of the single branch $(1/T_s)\log_2 M$. A brief schematic description is reported in Fig. 1.

The channel impulse response between the l-th LED and p-th PD is denoted as $g_{lp}[n]$. At discrete time n, the description of the signal filtered by the channel and receiving optical filters can be described as follows:

$$\begin{bmatrix} b_1[n] \\ b_2[n] \\ b_3[n] \end{bmatrix} = \mathbf{G}[n] * \begin{bmatrix} a_1[n] \\ a_2[n] \\ a_3[n] \end{bmatrix} \tag{1}$$

where $*$ denotes the discrete convolution operator and we have

$$\mathbf{G}[n] = \mathbf{C} \odot \mathbf{H}[n] \tag{2}$$

Optics EXPRESS

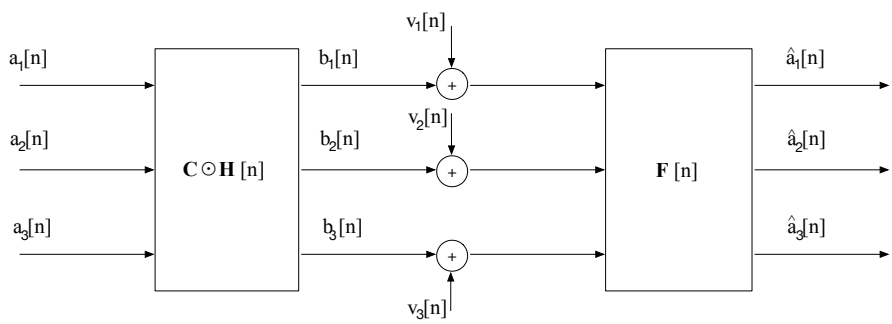

Fig. 1. Equivalent discrete MIMO system block diagram.

where $\odot$ denotes the Hadamard product. The 3×3 matrix $\mathbf{C}$ collects in the generic element c_{lp} the effect of the responsivity of photodiode and transmission of the optical filter tuned on p-th color with respect to the l-th LED. This can be evaluated as

$$c_{lp} = \frac{\int_{\lambda_{min}^{(T_l)}}^{\lambda_{max}^{(T_l)}} P_l(\lambda) T_p(\psi, \lambda) R_p(\lambda) d\lambda}{\int_{\lambda_{min}^{(P_l)}}^{\lambda_{max}^{(P_l)}} P_l(\lambda) d\lambda}, \tag{3}$$

where, $P_l(\lambda)$ is the power emitted at λ wavelength centered spectrum, $T_l(\psi, \lambda)$ is the transmission coefficient of filters and $R_p(\lambda)$ is the responsivity of the PDs. Hence, the best case is when $c_{lp} = 1, l = p$ and $c_{lp} = 0, l \neq p$, thus meaning that each PD is able to collect only the light coming from the reference LED and cross-talk is completely suppressed. Still related to (2), the generic element $h_{lp}[n]$ of the matrix $\mathbf{H}[n]$ represents time dispersion effects, that is, the memory of the channel. The well known channel model provided by Khan and Barry [16] describes the generic path that links any LED-PD pair and hence can be retained in our 3x3 MIMO channel, so that we can describe the behavior of the propagation with the superposition of a line-of-sight (LOS) component and a diffusive one. In particular $h_{lp}[n]$ is given by

$$h_{lp}[n] = \eta \delta[n - \Delta_{LOS}/T_s] + \frac{\zeta}{\tau_c} \exp\left(-\frac{n - \Delta_{Diff}/T_s}{\tau_c}\right) u(n - \Delta_{Diff}/T_s) \tag{4}$$

where the term η depends on the LOS component that is given by

$$\eta = \frac{(s+1)A_p}{2\pi d_{lp}^2} \cos^s(\phi_l) \cos(\psi_p) \tag{5}$$

In (5), s is the Lambertian emission order, given as $-\log_2[\cos(\phi_{\frac{1}{2}})]$, where $\phi_{\frac{1}{2}}$ is the LED's semi-angle at half-power. In (5), d_{lp} is the physical distance between the l-th LED and p-th PD, A_p is the physical area of the $p-th$ detector, ϕ_l is the angle of irradiance of the l-th LEDr, ψ_p is the angle of incidence to the p-th PD. Still related to (4), Δ_{LOS}/T_s is the T_s-sampled delay (we recall that T_s is the symbol period), of the LOS component, τ_c is the time-constant of the exponentially decaying diffuse channel, while ζ is the diffuse channel gain given by

Optics EXPRESS

$\zeta = (A_p/A_{room})\rho/(1-\rho)$ and A_{room} the area of the room while ρ is the average reflectivity of the room surfaces. Last, $u(.)$ is the Heaviside function.

Hence, in (2) the $\{l, p\}$-th discrete channel impulse response is:

$$g_{lp}[n] = \sum_{i=0}^{L-1} c_{lp} h_{lp}[n] \delta[(n-i)T_s] \tag{6}$$

where L is the length of the finite impulse response filter. Using a more compact notation, (1) becomes:

$$\mathbf{b}[n] = \mathbf{C} \odot (\mathbf{H} * \mathbf{a})[n] \tag{7}$$

where $\mathbf{H}[n]$ is the matrix of MIMO channel impulse responses. The ideal case of absence of cross-talk is described by $\mathbf{C}$ equal to the identity matrix, while in the most general case, $\mathbf{C}$ is not diagonal due to the imperfect optical color filtering applied at receiver side. This last aspect can be a result of low cost optical filters employment, and/or a color shift in the transmitted signal, which can happen when analog dimming is used or when the light beam reflects over colored surfaces, and/or LEDs with high wavelength occupancy leading to overlapping spectra and/or LEDs non-linearities. All these aspects can lead to cross-color (cross-talk) interference increase.

At the receiver, the signal is impaired also by the thermal noise as:

$$\mathbf{x}[n] = \mathbf{b}[n] + \mathbf{v}[n] \tag{8}$$

where $v_p[n]$ is the Additive White Gaussian Noise (AWGN) with zero mean and variance equal to σ_p^2 and statistically independent of the symbols.

3. Space-time equalizer

An estimate of the transmitted symbols is performed by filtering the received discrete signals:

$$\hat{\mathbf{a}}[n] = (\mathbf{F} * \mathbf{x})[n] \tag{9}$$

where $\mathbf{F}[n]$ is the matrix of equalizer impulse responses, with 3×3 FIR filters, where the rows span all the LEDS, for $l = 1, 2, 3$, and the columns span all the PDs, for $p = 1, 2, 3$:

$$\mathbf{F}[n] = \begin{bmatrix} f_{11}[n] & f_{12}[n] & f_{13}[n] \\ f_{21}[n] & f_{22}[n] & f_{23}[n] \\ f_{31}[n] & f_{32}[n] & f_{33}[n] \end{bmatrix} \tag{10}$$

The estimation error is defined as:

$$e_l[n] = a_l[n] - \hat{a}_l[n] = a_l[n] - \sum_{p=1}^{3} \sum_{k \in \mathcal{S}_{lp}} f_{lp}[k] x_p[n-k] \tag{11}$$

where $\mathcal{S}_{lp}$ is the finite set that collects the indexes of the equalizer coefficients for the estimation of the symbol emitted by the $l-th$ LED at time n, for $p \in \{1, 2, 3\}$. In order to find the optimal equalizer we minimize the mean-square error (MSE) $J(\mathbf{F})$:

$$J(\mathbf{F}) = \mathrm{E}\left\{\mathbf{e}^T[n]\mathbf{e}[n]\right\} = \sum_{l=1}^{3} \mathrm{E}\left\{e_l[n]^2\right\} = \sum_{l=1}^{3} J_l(\mathbf{f}_l) \tag{12}$$

where $\mathbf{f}_l$ is the vector representing the l-th row of the $\mathbf{F}$ matrix.

Optics EXPRESS

We have that it is possible to either minimize $J(\mathbf{F})$ or minimize each $J_l(\mathbf{f}_l)$, independently. To find the optimal Wiener filters coefficients the gradient of every $J_l(\mathbf{f}_l)$ should be imposed to zero:

$$\frac{\partial J_l(\mathbf{f}_l)}{\partial f_{lq}[m]} = -2\mathrm{E}\left\{e_l[n]x_q[n-m]\right\} = \mathbf{0}, \forall q \in \mathcal{S}_{lp}, \forall l = 1,2,3 \tag{13}$$

Let us rewrite the normal equations (13) as follows:

$$\begin{aligned}
\mathrm{E}\left\{e_l[n]x_q[n-m]\right\} &= \mathrm{E}\left\{\left(a_l[n] - \sum_{p=1}^{3}\sum_{k\in\mathcal{S}_{lp}} f_{lp}[k]x_p[n-k]\right)x_q[n-m]\right\} \\
&= \mathrm{E}\left\{a_l[n]x_q[n-m]\right\} - \mathrm{E}\left\{\sum_{p=1}^{3}\sum_{k\in\mathcal{S}_{lp}} f_{lp}[k]x_p[n-k]x_q[n-m]\right\} \\
&= R_{a_l,x_q}[m] - \sum_{p=1}^{3}\sum_{k\in\mathcal{S}_{lp}} f_{lp}[k]R_{x_p,x_q}[m-k] = 0
\end{aligned} \tag{14}$$

Finally, let us rewrite (14) in the classical Wiener form:

$$\sum_{p=1}^{3}\sum_{k\in\mathcal{S}_{lp}} f_{lp}[k]R_{x_p,x_q}[m-k] = R_{a_l,x_q}[m]. \tag{15}$$

3.1. Adaptive MISO equalizer

Let us observe that the 3×3 MIMO system can be analyzed as three equivalent 3×1 multiple-input-single-output (MISO) systems, thus the estimation of the signal emitted by the $l-th$ LED can be treated independently from the other two branches.In Fig. 2 the block diagram of the adaptive equalization scheme is shown.

The simplest adaptive algorithm for calculation of the Wiener filter when the statistics of the signals (e.g. $R_{a_l,x_q}[m]$) are unknown is the Least Mean Squares (LMS) algorithm that belongs to the stochastic gradient methods [18]. The way used to update the filters' coefficients at the i-th step is described by the following relationship:

$$f_{lp}^{(i)}[n] = f_{lp}^{(i-1)}[n] - \mu_{lp}\ e_l[n]x_p[n], \qquad \forall l = 1,2,3,\ \forall p = 1,2,3 \tag{16}$$

where the generic term μ_{lp} is the learning factor of the equalizer and $f_{lp}^{(0)}[n] = \delta[n]$.
In this regard, when symbols $a_l[n]$ reported in Fig. 2 are not known at receiver, the adaptive algorithm is *blind* if the Decision Directed (DD) technique is used and the reference $a_l[n]$ is obtained through hard detection of the equalized signal $\hat{a}_l[n]$. Alternatively, the equalizer is *semiblind* when, before applying the DD technique, initial synchronization symbols are used to train the LMS algorithm (16).

3.2. Filter support design

When the channel cross-talk interference is present, equipping each branch after the PD with of a time-based equalizer may not be able to counterbalance the residual interference due to possible imperfect color interference suppression acted by optical filters. For this reason in this contribution we investigate the use of a multichannel equalizer. The adoption of a space-time equalizer can of course increase the computational complexity; however, in this work we explore

Optics EXPRESS

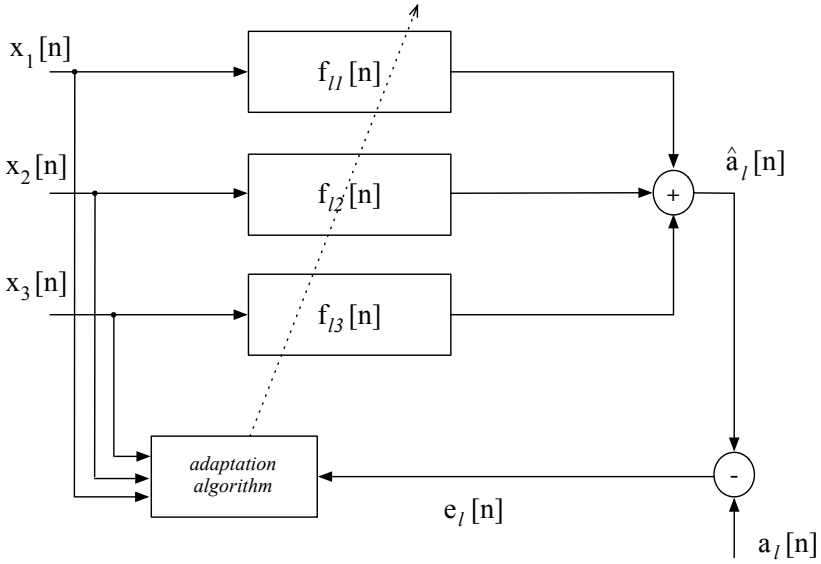

Fig. 2. Equivalent MISO model for the equalizer.

the opportunity of having an equalizer f_{lp} that presents impulse responses of different length, depending on the value of l, trying to reduce the computational complexity. Specifically, when $l \neq p$, $\mathcal{S}_{lp}$ can have a significantly shorter length, because, due to the color optical filters, the interference attenuation is higher. In other words, the delayed pulses that produce time intersymbol interference are more attenuated. As will be shown in the numerical result section, this filter design choice will also lead to have an equalizer that reaches convergence even when transmitted symbols references are not available at the receiver, and reduce the convergence time.

4. Numerical results

In order to validate our spatial-temporal MIMO equalizer we consider VLC channel impulse responses as those presented in [19], which are reported as example of VLC-to-PD channel in Figs. 3 and 4. The channel FIR considered in the simulations are highlighted with red circle stem. To evaluate the spatial intersymbol interference of the system, we use two different settings for the cross channel interference that are related to the case of using two different optical filters. The first one we consider presents very small transient bandwidth ($\mathbf{C}_1$) while the second one has worse out of band filtering performances ($\mathbf{C}_2$), which is the case of having optical filters with different quality [7] as we report in the following:

$$\mathbf{C}_1 = \begin{bmatrix} 0.85 & 0.15 & 0 \\ 0.15 & 0.7 & 0.15 \\ 0 & 0.15 & 0.85 \end{bmatrix} \tag{17}$$

$$\mathbf{C}_2 = \begin{bmatrix} 0.7 & 0.2 & 0.1 \\ 0.25 & 0.65 & 0.1 \\ 0.05 & 0.15 & 0.8 \end{bmatrix} \tag{18}$$

However both color filtering are far from being ideal since, for example, the out-of-diagonal elements describe the amount of cross-talk, hence the ratio between main path (diagonal) and

Optics EXPRESS

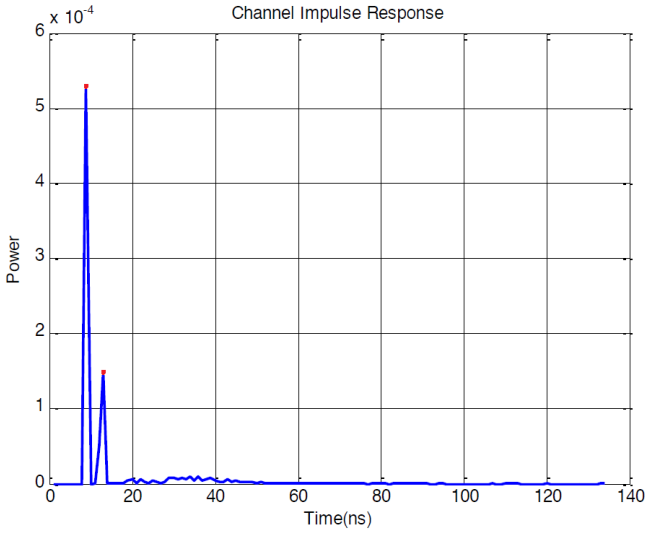

Fig. 3. Channel impulse response in the case of an open office room with human bodies [19].

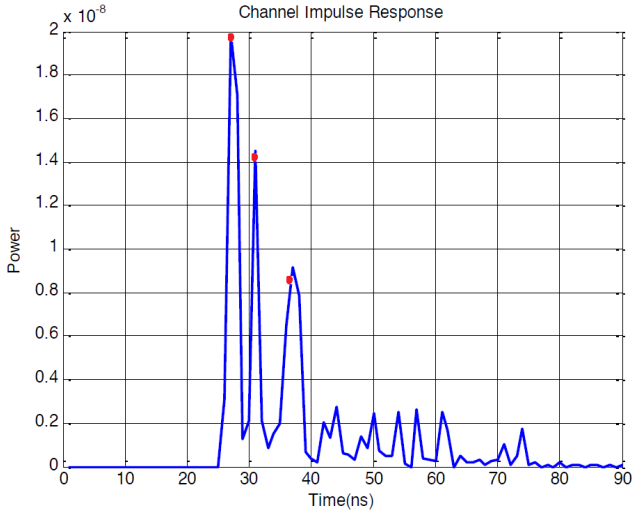

Fig. 4. Channel impulse response in the case of a factory environment, higher multipath [19].

out-of-diagonal, can represent the signal to interference ratio. This latter does not exceed 7.5dB (for $\mathbf{C}_1$) and 6dB (for $\mathbf{C}_2$). The 3 LEDs we considered present a modulation bandwidth of 160MHz that is the same bandwidth of the 3 PDs. The symbol time is 5ns and modulation format is 4-ASK so the whole transmission rate is 960Mb/s. The transmitter and receiver pitch is 3cm while the full width at half maximum of the transmitter is 60°and the field of view of the detector is 90°, the lenses concentrate the light within a 60°beam. If not different specified, the SNR in the simulations is equal to 23 dB corresponding to an emitting power of 1 W and distance between transmitter and receiver of 2.9 m. To explain better, the distance we reported is that from green LED, in the middle between red and blue, and the central PD having a green

Optics EXPRESS

filter in front of it. We refer for modeling moth LEDs and PDS to the ones used in [8], Luxeon Star Rebel for LEDs and Vishay BPW34. Moreover, 5 synchronization symbols are used for training the semiblind equalizer and the μ_{lp} learning factor is set to 10^{-3}. The next figures report Symbol Error Rate (SER), averaged over 5000 MonteCarlo runs. In Fig. 5 and 6 we show SER performance comparison between the single channel equalizer (Time Equalizer (TE)), and the multichannel equalizer (Space-Time Equalizer (STE)).

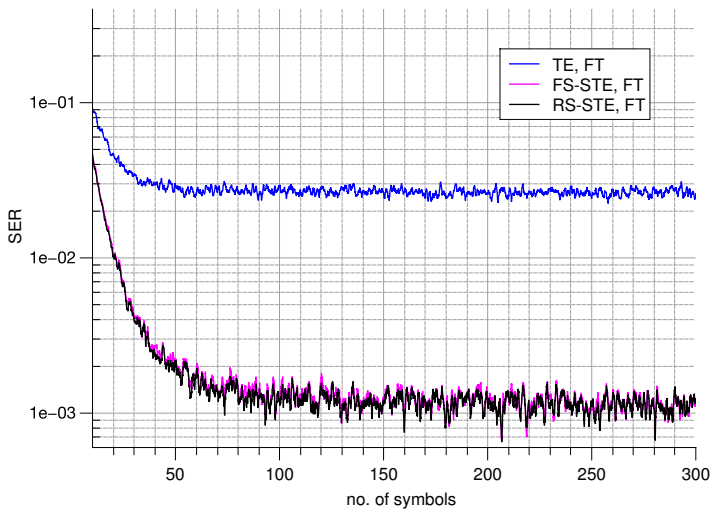

Fig. 5. Evolution of SER in the first 300 symbols received when the FT is used. The optical channel scenario is given by $\mathbf{C}_2$ as the effective responsivity, and $\mathbf{H}_1$ for the impulse response.

In this latter case we distinguish between Full Size-STE (FS-STE), in which the filter support $\mathcal{S}_{lp}$ has the same size for every $p = \{1, 2, 3\}$ ($p = 1$ means red, $p = 2$ means green and $p = 3$ means blue), over Reduced Size-STE (RS-STE) where $\mathcal{S}_{lp}$ has fewer elements when $p \neq l$. Specifically, the number of coefficients of RS-STE is 2×4 lower than FS-STE.

In order to highlight the effect of filters' coefficients update and how it impacts on detection errors, we plotted SER over symbols received so as to emphasize the convergence properties of the proposed equalizer. The obtained SER curves are compared with the ideal Fully Trained (FT) equalizer. Since all the symbols are used for training [21], the FT equalizer has not practical relevance; nevertheless, its accuracy (SER) constitutes a lower bound for this family of equalizers so that it can be correctly employed in benchmarking and performance comparison.

Fig. 5 refers to to the case of $\mathbf{C}_2$ and channel impulse response as in Fig. 3, TE, FS-STE and RS-STE are compared when reference symbols are available at the receiver side (FT case). It is worth noting that both FS-STE and RS-STE have better performance than TE. Moreover the difference between FS-STE and RS-STE is minimal and both equalizers converge to the same SER values. Specifically, after receiving 300 symbols the TE reaches SER of 2.5×10^{-2}, instead RS-STE and FS-STE are close to reach 10^{-3}. Thus, it is fundamental noting that applying a STE allows the use of space dimension (color in this case) so the decision is based on a bi-dimensional space rather than a single one as in the TE case and this leads to a SER decrease. In fact, the STEs utilize spatial dimension in order to tackle the residual crosstalk while for TE cross-talk is noise that cannot be mitigated. Furthermore the reduction of coefficients in the multichannel equalizer (RS-STE), when $l \neq p$, leads to a reduction in computational complexity without compromise the communication performances.

Under the same optical channel conditions of Fig. 5, in Fig. 6 we consider the case of blind

Optics EXPRESS

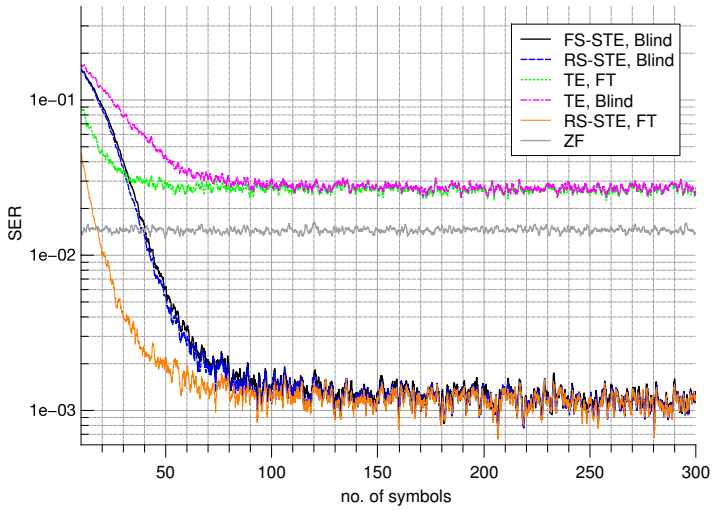

Fig. 6. Evolution of SER in the first 300 symbols received. The optical channel scenario is given by $\mathbf{C}_2$ as the effective responsivity, and $\mathbf{H}_1$ for the impulse response. In the figure the Blind equalizers are compared with the FT cases and the ZF equalizer.

equalization. The FT case (red curve) is shown as a performance reference. As in the previous figure, STE outperforms TE. In this case it is possible to see that having reduced the number of coefficients in RS-STE, slightly increases the algorithm speed of convergence without compromise the SER reached after 300 symbols, equal to 10^{-3}. In this scenario, without training symbols the convergence is reached at the 80-th symbol instead of the 60-th of the FT case, in particular the blind FS-STE is slighting slower than the blind RS-STE.

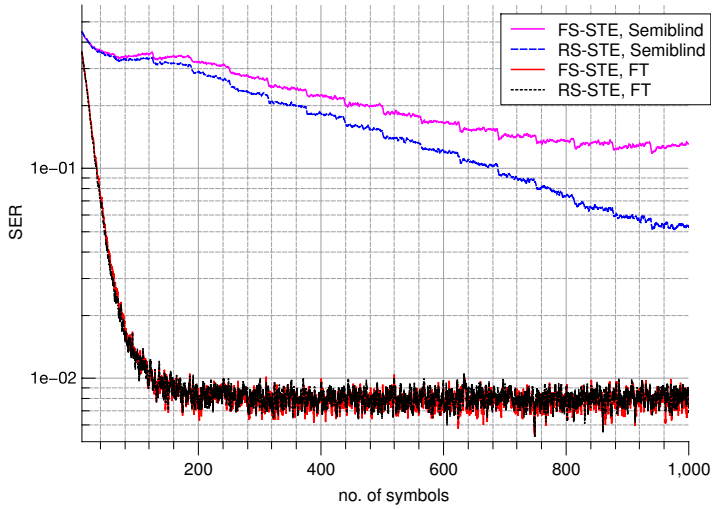

Fig. 7. Evolution of SER in the first 1000 symbols received. The optical channel scenario is given by $\mathbf{C}_2$ as the effective responsivity, and $\mathbf{H}_2$ for the impulse response. In the figure the Semiblind equalizers are compared with the FT cases.

Optics EXPRESS

Moreover, in Fig. 7 a scenario with higher temporal intersymbol interference is evaluated, namely the case of $\mathbf{C}_2$ and propagation environment as for Fig. 4. Semiblind RS-STE and FS-STE are compared and it is shown that in this case SER performance gap between FT and semiblind equalizers is substantial. In fact, FT FS-STE reached SER of 9×10^{-3} after 1000 symbols, semiblind RS-STE 5×10^{-3} and FS-STE 5×10^{-2}. Thus it is possible to infer that the RS-STE has a more robust behavior over FS-STE when few reference symbols are available and the interference is high, along with the benefit of being less computational complex. Last, both TE

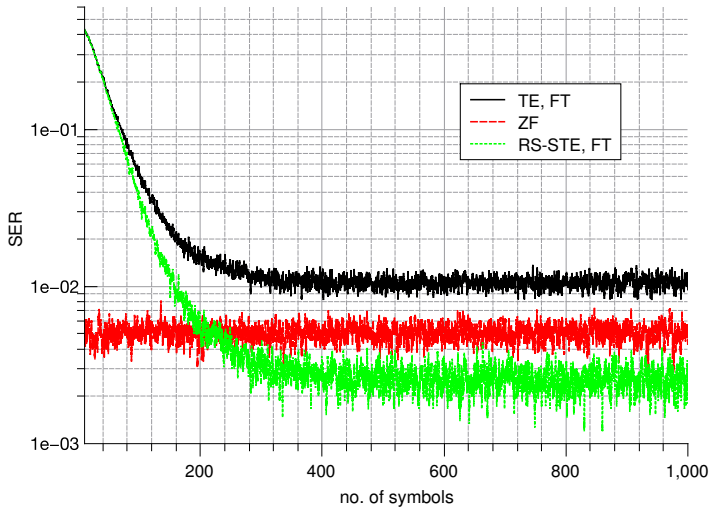

Fig. 8. Evolution of SER in the first 1000 symbols received when the FT is used. The optical channel scenario is given by $\mathbf{C}_1$ as the effective responsivity, and $\mathbf{H}_2$ for the impulse response.

and STE are compared with the zero-forcing (ZF) equalizer developed for ASK modulation in RGB transmission in [8]. In order to provide an unfair comparison for our technique, only for ZF, we assume to be in the case of perfect channel knowledge at the receiver. The simulation scenario considered in Fig. 8 is $\mathbf{H}_2$ and $\mathbf{C}_1$. It is possible to see that the STE reaches lower SER than TE and ZF. Moreover, when the channel cross talk interference is higher, the advantage in the use of STE is even more evident, as is the case of Fig. 6 where ZF reaches SER of only 0.5×10^{-2} in comparison with 10^{-3} of FT STE. Last, in Fig. 9 we report the performance of RS-STE, TE and ZF have been reported. We take into account the SER achieved after a transitory of 800 symbols so as to show the limit performance. We change the transmitting power in order to increase the SNR and this can be considered as having different distances between transmitter and receiver. We refer to the channel characterized by channel impulse response as in the case of $\mathbf{H}_2$ with color filtering characterized by $\mathbf{C}_2$. It is important noting that the ZF equalizer can achieve a SER of the order of 2.6×10^{-2} at a SNR of 23dB. On the other hand the TE presents performances that are a bit better since at 23dB achieves 1.9×10^{-2}. The SER obtained with RS-STE is one order of magnitude lower and this gain can be also seen in a horizontal sense. This means that RS-STE is able to obtain the same SER of TE wth a 5dB lower that corresponds to move the receiver 2 more meters far from the transmitter. Although the asymptotical BER is around 10^{-3} we need to remark two important aspects. First, the performance we evaluated refers to low signal-to-interference-noise ratio and this can be inferred by looking at the coefficients of color filter matrices. Second, the achieved BER for the uncoded case allows to achieve error-free communications when, for example, polar codes are used as in [22].

Optics EXPRESS

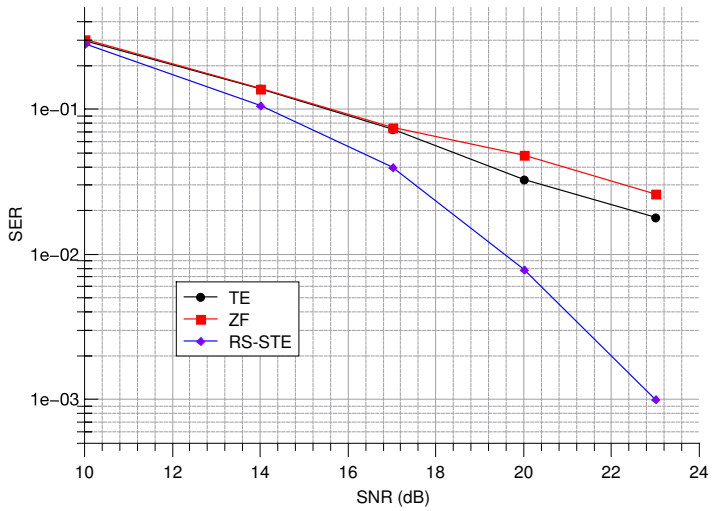

Fig. 9. SER-vs.-SNR when the optical channel scenario is given by $\mathbf{C}_2$ and $\mathbf{H}_2$

5. Conclusion

In this paper we addressed the issue of channel cross-talk interference in color-based VLC diversity transmission schemes. We evaluated the VLC channel equalization when ISI is present in both color (space) and time domain, showing that using a multichannel equalizer leads to better interference suppression with respect to a time-domain only equalizer. We investigated a blind adaptive equalization with a flexible filter's coefficients complexity, whose computational complexity changes in regards to the quality of the optical front-ends used, e.g. it requires more filters coefficients only when high cross-channel interference is present.